# APPLICATON OF DESIGN OF EXPERIMENTS (DOE) ON THE PROCESSING OF RAPID PROTOTYPED SAMPLES

J.Weinmann, H. Ip, D. Prigozhin, E. Escobar, M. Mendelson, and R. Noorani

National Science Foundation
Research Experience for the Undergraduates Program
Loyola Marymount University
Los Angeles, CA

**Abstract**

The purpose of this experiment was to improve the Fused Deposition Modeling Process by examining the tensile strength of samples fabricated in a Stratasys FDM 1650 Machine utilizing the methods of Design of Experiments. A two-level, four-factor, full factorial experiment was conducted. The selected factors were temperature, air gap, slice thickness, and raster orientation. A regression equation determined the level each factor should be set in order to optimize the FDM machine settings. It was found that single factors - small air gap, small layer thickness and low raster orientation, as well as the interaction between high temperature and small layer thickness yielded the greatest effect the response.

## 1. Introduction

Fused deposition modeling (FDM) is a process that is used for fabricating solid prototypes from a computer-aided design (CAD) data file [1]. The process fabricates 3-D parts from a build-up of 2-D layers. In this process, an Acrylonitrile-Butadiene-Styrene (ABS) thermoplastic polymer is extruded through a heated nozzle to deposit the layers. In a previous paper, we showed that the orientation of the layers created anisotropic tensile properties [2]. Other investigators have also experienced similar results [3].

Previous investigators have used design of experiments (DOE) as a method to maximize strengths of the FDM-processed specimens of silicon nitride [4] and ABS polymer [3]. Many of the factors used for influencing the strength were entirely different in these studies. These investigators have not physically interpreted their selected factor levels in terms of the material properties and microstructure.

The purpose of this paper is to use quality engineering tools to design, analyze and physically interpret our selection of the FDM processing factors and their levels.

## 2. Experimental Methods

The 12-step design process was used for our experimental [5]. First, the problem of concern was the low strength of FDM-processed ABS test specimens; second, our objective was to maximize the tensile strength; third, the yield and ultimate strengths were selected as the quality characteristics, i.e., the response; fourth, the factors were determined by team brainstorming and were recorded on a cause-effect diagram [6]; fifth, four factors and no-noise factors were selected for our study; and sixth, a two-level experiment was selected.

Seventh, an L16 ($2^4$) full-factorial experiment was used for the DOE; eighth, all of the selected factors could potentially interact with each other; ninth, all of the interactions were listed; tenth, the trials were randomized and three replications per trial were used; eleventh, the column effects method and plots of the response vs. the effects of factors and interactions were used to analyze the data; and twelfth, the 95% statistically significant factors and interactions were identified. Our results were interpreted in terms of fracture behavior and microstructure to validate our results.

A Stratasys FDM-1650 modeling machine was used to fabricate the test specimens. The materials were ABS P400 build material and the support material [1]. Each material was in the form of a filament that was fed into a heated extrusion head to form a semi-liquid polymer. The polymer was deposited at locations on the X-Y plane according the part requirements in the STL file. The layer thickness was determined by the FDM Quickslice™ software. Then the head was moved vertically to deposit a new 2-D layer on top of the previous one. In this way, the 3-D solid model was built-up by multiple depositions of 2-D layers.

Each layer was formed by first depositing the perimeter (road width) around the X-Y plane of the test specimen design and then filled the inside of the perimeter with a raster pattern that had a preferred orientation. The layer bonded to the underlying structure. This process was similar to the 2-D lay-up of 90°/45° and 0°/45° laminate composites [7].

The design of the test specimens was in the shape of a dog-bone, similar to ASTM D638-97. However, the width of the gauge section in the test specimen was reduced to 8.13 mm (0.320 in.), because some specimens had failed outside the gauge length. The gauge length was 68.8 mm (2.71 in.) long and had a constant thickness of 3.18 mm (0.125 in.). The overall length of the specimens was 127 mm (5.0 in.). The 0° fibers were oriented along the length of the samples, parallel to the tensile direction.

The specimens were tested in tension by an Instron 4505 universal testing machine. The cross-head speed of the test machine was 0.0212 mm/s. Strain was measured with an extensometer, and the stress vs. strain curves were plotted. The yield stress was measured at 0.2% offset strain, and the ultimate strength was measured at the maximum tensile stress.

A microscopic analysis of the fracture surfaces in the tensile samples was conducted at magnifications ranging from 6.5X to 45X. Pair wise comparisons of the samples were conducted in such a way that only one factor level was varied between the pair.

## 3. Design of Experiment

A cause-effect diagram was used to list the possible causes affecting the tensile strength of the test specimens. Some of the possible causes were the build specifications (road width, air gap, layer thickness, raster orientation), machine environment (model temperature), and ABS material (density). Four factors were selected for this experiment: (A) model temperature, (B) air gap, (C) layer thickness, and (D) raster orientation at two levels, i.e., low (-1) and high (+1), as shown in **Table 1**. An L16 ($2^4$) experimental design was utilized as shown in **Table 2**. The mean tensile strength data, $\overline{Y}_{yield}$ and $\overline{Y}_{ultimate}$, are shown for the yield and ultimate strengths, respectively.

| Parameter (Factor) | Description | Low Level (-1) | High Level (+1) |
|---|---|---|---|
| A | Temperature | 268˚C | 277˚C |
| B | Air Gap | -0.0254 mm | 0 mm |
| C | Layer Thickness | 0.254 mm | 0.356 mm |
| D | Raster Orientation | 0˚/45˚ | 90˚/45˚ |

**Table 1.** Factors and Levels

| Trial | A | B | C | D | $\overline{Y}_{yield}$ (MPa) | $\overline{Y}_{ultimate}$ (MPa) |
|---|---|---|---|---|---|---|
| 1 | 268˚C | -0.0254 mm | 0.254 mm | 0˚/45˚ | 15.70 | 16.31 |
| 2 | 268˚C | -0.0254 mm | 0.254 mm | 90˚/45˚ | 12.62 | 13.64 |
| 3 | 268˚C | -0.0254 mm | 0.356 mm | 0˚/45˚ | 11.99 | 12.86 |
| 4 | 268˚C | -0.0254 mm | 0.356 mm | 90˚/45˚ | 9.06 | 10.36 |
| 5 | 268˚C | 0 mm | 0.254 mm | 0˚/45˚ | 12.97 | 13.38 |
| 6 | 268˚C | 0 mm | 0.254 mm | 90˚/45˚ | 12.98 | 13.81 |
| 7 | 268˚C | 0 mm | 0.356 mm | 0˚/45˚ | 11.91 | 12.83 |
| 8 | 268˚C | 0 mm | 0.356 mm | 90˚/45˚ | 7.67 | 8.77 |
| 9 | 277˚C | -0.0254 mm | 0.254 mm | 0˚/45˚ | 17.56 | 17.77 |
| 10 | 277˚C | -0.0254 mm | 0.254 mm | 90˚/45˚ | 18.70 | 19.00 |
| 11 | 277˚C | -0.0254 mm | 0.356 mm | 0˚/45˚ | 10.31 | 11.39 |
| 12 | 277˚C | -0.0254 mm | 0.356 mm | 90˚/45˚ | 9.17 | 10.35 |
| 13 | 277˚C | 0 mm | 0.254 mm | 0˚/45˚ | 13.70 | 13.90 |
| 14 | 277˚C | 0 mm | 0.254 mm | 90˚/45˚ | 12.53 | 13.64 |
| 15 | 277˚C | 0 mm | 0.356 mm | 0˚/45˚ | 10.60 | 11.36 |
| 16 | 277˚C | 0 mm | 0.356 mm | 90˚/45˚ | 6.67 | 8.83 |

**Table 2.** L16 ($2^4$) Experimental Design Report

## 4. Analysis of Data

Based on the results in **Table 2**, the column effects for factors A, B, C, D and their interactions were determined for both yield and ultimate strengths. The analysis of the effects on the response was plotted in **Figs. 1 and 2**. The ~95% (±2σ) confidence interval for the standard error of the effects [8] of each factor was calculated to be ±0.73 MPa. When the response lies outside this interval, the effect is significant; and the converse is true when the effects are inside the interval.

In **Fig. 1,** factors B (air gap), C (layer thickness), D (raster orientation), and interaction AC lay outside the 95% confidence interval 12.13 ± 0.73 MPa, which indicates only these factors and interaction have significant effect on yield strength. **Fig. 2** shows the detailed analysis of the AC interaction. The conclusion from these figures is that to maximize the yield strength, the low-level of factors B, C and D, and the interaction of high-level A and low-level C should be selected.

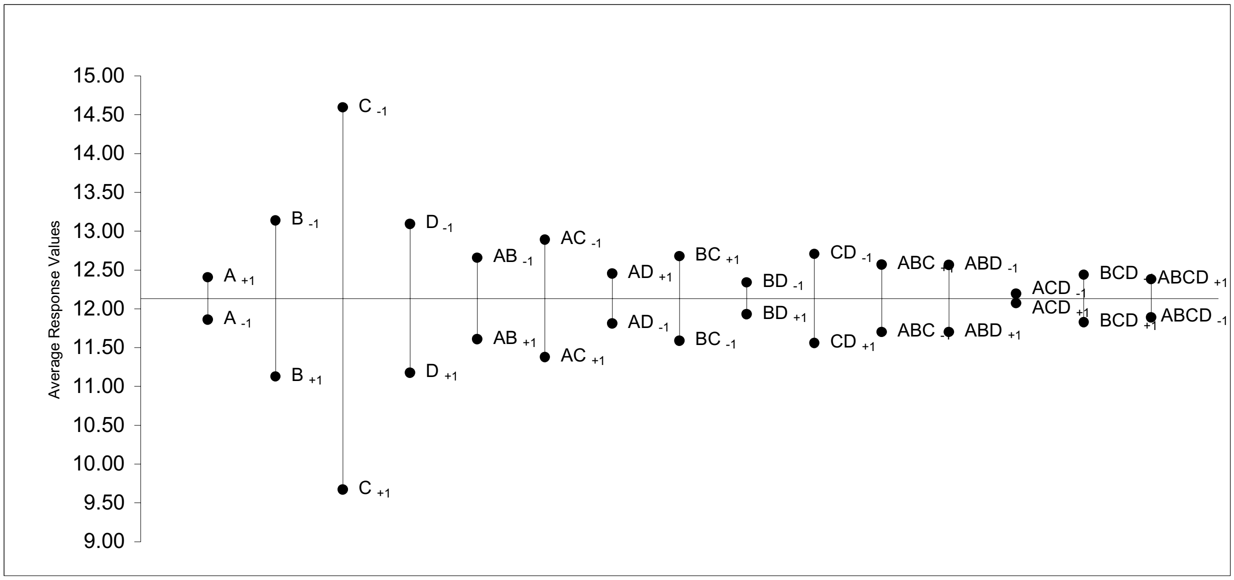


**Fig. 1.** Yield Strength Response (MPa) vs. Effects of Factors/Levels

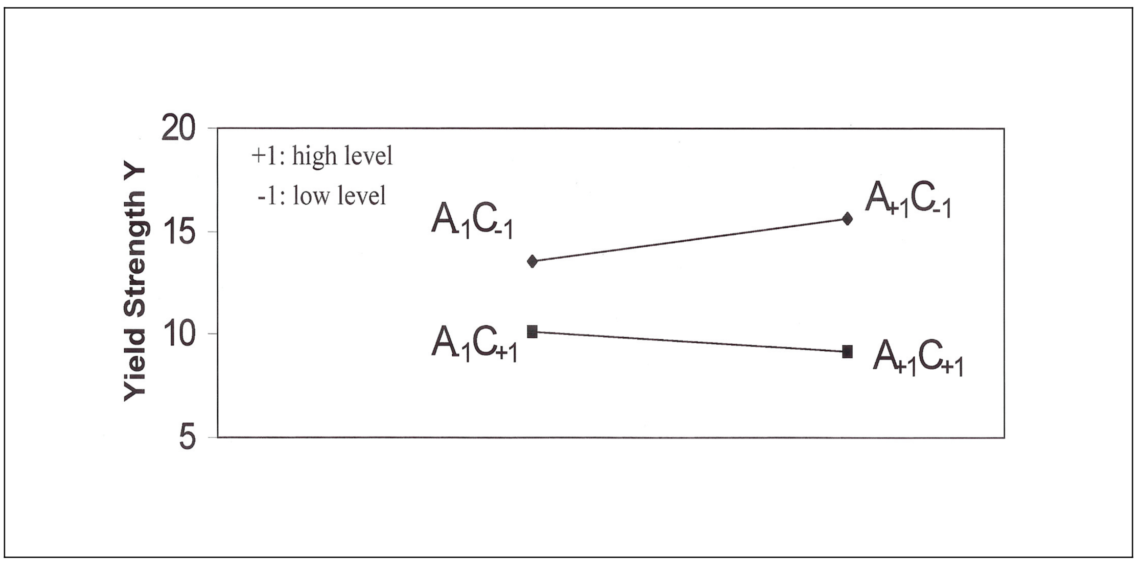


**Fig. 2.** Interaction between Temperature (A) and Layer Thickness (C) on Yield Strength

In **Fig. 3**, only factors B (air gap) and C (layer thickness) lay outside the 95% confidence interval 13.01 ± 0.73 MPa. Therefore, these are the only factors that have significant effects on ultimate strength. In order to achieve maximum ultimate strength, the low-level of factors B and C should be selected.

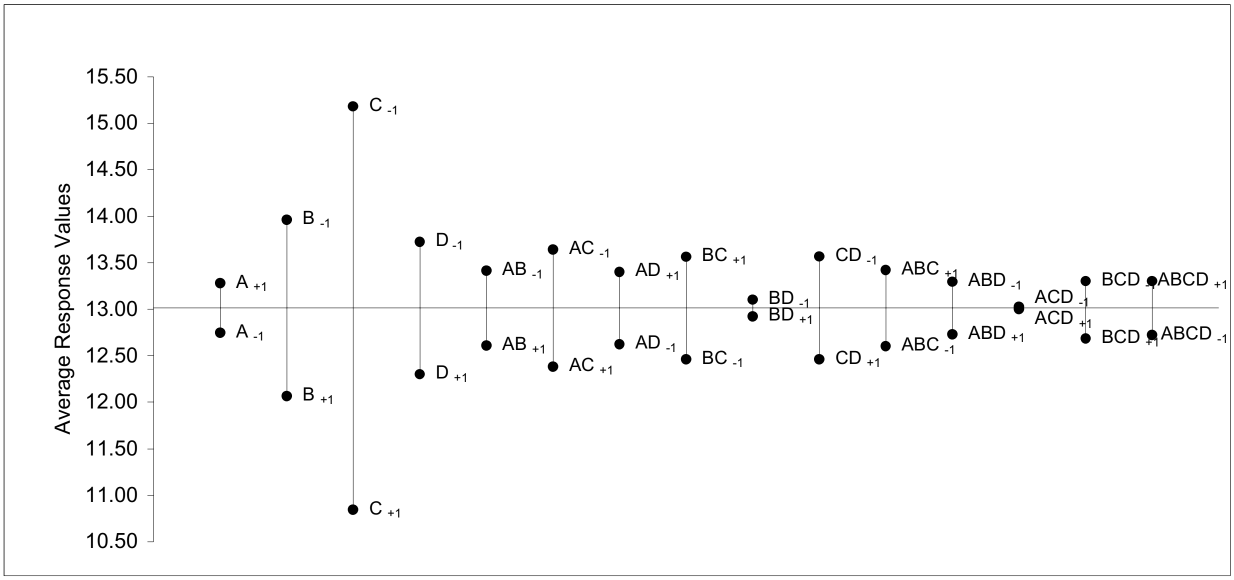


**Fig. 3.** Ultimate Strength Response (MPa) vs. Effects of Factors/Levels

In order to verify the above results, a regression equation was used to predict different factor levels and two-factor interactions that maximized the strength response, ŷ [9]:

$$\hat{y} = \beta_o + \Sigma_i \beta_i x_i + \Sigma_i\Sigma_j \beta_{ij} x_I * x_j = \beta_o + \beta_B x_B + \beta_C x_C + \beta_D x_D + \beta_{AC} x_{A+1} * x_{c-1} \qquad (1)$$

Here $x_i$ represents factors B, C and D which take on ±1 values for the low/high levels that will maximize tensile strength. Also, $x_i * x_j$ represents the interaction of $A_{+1} * C_{-1}$ that takes on ±1 values. The values of the β coefficients are shown in **Table 3**. Coefficient $\beta_o$ represents the intercept (or mean value of Y). Coefficients $\beta_i$ are the slope of multiple regression for factors B, C and D. $\beta_{AC}$ represents the coefficient that is associated with the A*C interaction. Here the coefficients are one-half the effects of each factor and interaction in **Figs. 1** and **3.** The values of the coefficients are shown in **Table 3**.

| Tensile Strength (MPa) | Coefficients | | | | |
|---|---|---|---|---|---|
| | $\beta_0$ | $\beta_B$ | $\beta_C$ | $\beta_D$ | $\beta_{AC}$ |
| Yield | 12.13 | -1.01 | -2.46 | -0.96 | -0.76 |
| Ultimate | 13.01 | -0.95 | -2.17 | -- | -- |

**Table 3.** Calculated Coefficients for B, C, D Factors and Interaction AC in Eq. (1).

Eq. (1) verifies that for maximum yield strength, factor levels should be $B_{-1}$, $C_{-1}$, $D_{-1}$, and $A_{+1}C_{-1}$. For maximum ultimate strength, the factor levels should also be $B_{-1}$ and $C_{-1}$.

When the interaction effects are moderate (see **Fig. 2**), errors can result in selecting the factor levels if the interactions are not taken into account. For example, in previous work [4], all of the columns in their 3-level experimental design were filled with main factors. This created a lower resolution experimental design, where the interactions and their aliases could not be analyzed. In this case, Eq. (1) would become an additive response of main factors, where $\Sigma_i\Sigma_j \beta_{ij} x_i * x_j = 0$. When our interactions were analyzed, $A_{+1}C_{-1}$ was preferred over $A_{-1}C_{-1}$.

## 5. Physical Interpretation

The selected process factor levels must physically make sense from the point of view of the structural properties and microstructure of ABS polymer. The yield strength was correlated with stretching the polymer chains and viscoelastic flow of ABS, and the ultimate strength was correlated with fracture initiation through the ABS structure [7]. Once a critical crack length was initiated, it propagated either at 45° or 90° to the tensile axis depending upon the raster orientation.

The FDM machine deposited the raster patterns at 0°/45° and 90°/45° oriented composite structures. The weak interfacial bonding between the oriented fibers can be caused by (1) weak interlaminar shear properties of the fibers, (2) the volume change during the ABS transformation from liquid to solid, or (3) formation of pores during FDM processing [2].

Factor B – Air Gap: When the air gap was set at a negative value, the adjacent fibers overlapped each other. This increased the bonding between the fibers and created a tighter structure, as the porosity between the fibers was reduced. The lower porosity composite is expected to translate into a higher tensile strength. Hence, it is reasonable that a lower air gap setting ($B_{-1}$) would maximize the composite strength.

Factor C – Layer Thickness: When the layer thickness was reduced, the fiber diameter was reduced, and the fiber shape became more oval as shown in **Fig. 5**. Also, the $0^o$ fibers (light phase) overlapped each other to a greater extent when the layer thickness was low. The lower layer thickness reduced the porosity and increased the volume fraction of fibers (to a smaller extent), which strengthened the overall composite structure. This adequately explains why a low layer thickness ($C_{-1}$) is selected for increasing the tensile strength.

Factor D – Raster Orientation: When the two raster orientations were compared, the difference between them was in the $0^o$ and $90^o$ oriented fibers since the $45^o$ layers acted similarly in both cases. Fibers oriented parallel to the tensile axis would exhibit maximum strength, while those oriented perpendicular to it would have their weakest strength. This is shown in **Fig. 4** where the $90^o/45^o$ structure fibers perpendicular to the tensile axis. However, the $0^o/45^o$ structure was strong along the $0^o$ axis, and fracture was along the weaker $45^o$ fiber interfaces, where the interlaminar sheer stress was high. Therefore, $0^o/45^o$ structures are expected to have a higher tensile strength than $90^o/45^o$ structures. It is logical to select $D_{-1}$ factor level for maximizing the tensile stress.

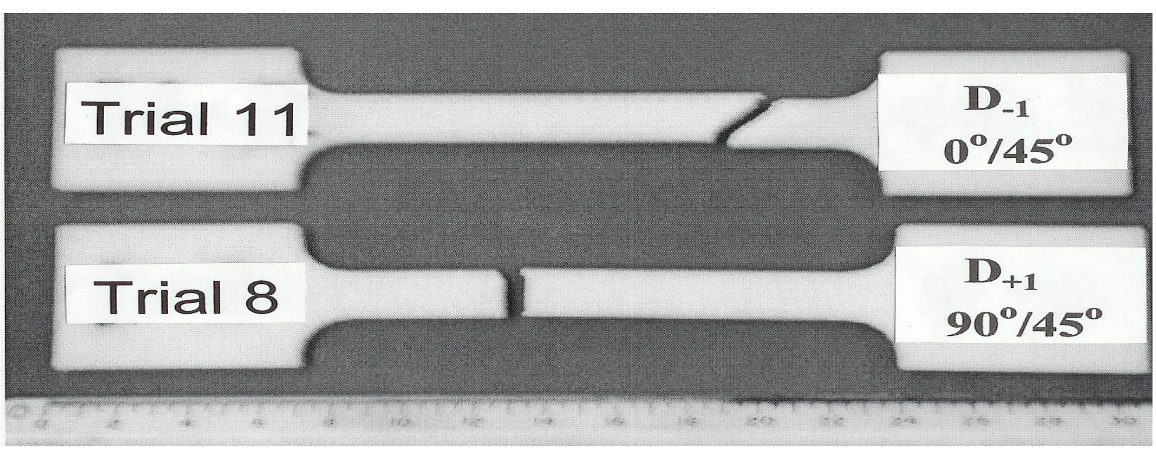


**Fig. 4**. Fracture of Tensile Specimens

AC Interaction: The high temperature allowed a longer time for viscous flow of the ABS material to fill the open porosity. It also contributed to a greater degree of bonding between the fibers. Hence, it would be expected that the higher temperature ($A_{+1}$) would increase the tensile strength. As previously explained, the low layer thickness ($C_{-1}$) setting was preferred for increasing the tensile strength. Therefore, it is not surprising that the high temperature and low layer thickness ($A_{+1}C_{-1}$) would interact to maximize the tensile strength.

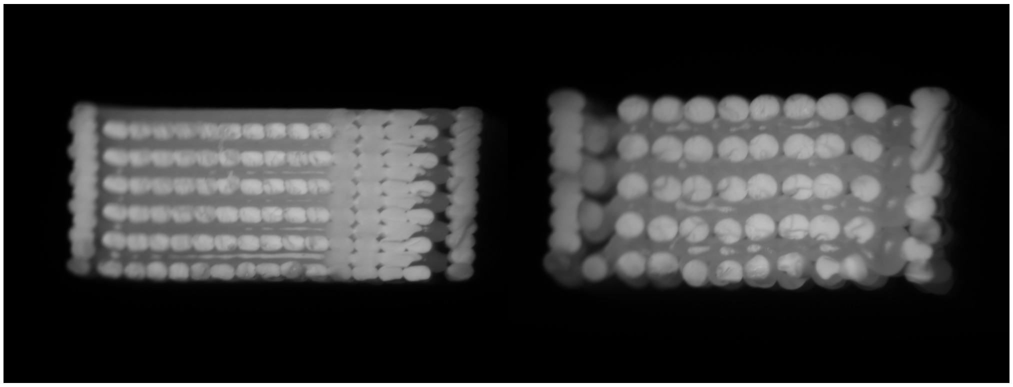

**Fig. 5.** Trial 9 (Left) and Trial 11 (Right)
Trial 9: Fracture surface of $0^o/45^o$ composite at low layer thickness.
Trial 11: Fracture surface of $0^o/45^o$ composite at high layer thickness.

## 6. Conclusions

Using an L16 ($2^4$) full factorial experimental design, the following conclusions resulted from our work:

1. The yield strength is maximized by low air gap, low layer thickness, low raster orientation and the interaction between high mold temperature and low layer thickness.
2. The ultimate strength is maximized by low air gap and low layer thickness.
3. The effects of the factor levels on tensile strength were explained in terms of their microstructure and processing.


**Acknowledgment**

The work was funded by a National Science Foundation (NSF) grant to Loyola Marymount University for the Research Experience for Undergraduates (REU) program.


## References


[1] Stratasys, FDM-1650 modeling machine, system documentation, web site: http://www.stratasys.com.

[2] Es-Said, O., Noorani, R., Mendelson, M., Foyos, J., and Marloth, R. (2000), "Effect of Layer Orientation on Mechanical Properties of Rapid Prototyped Samples," *Materials and Manufacturing Processes*, 15 [1], 107-122.

[3] Montero, M., Roundy, S., Odell, D., Ahn, S-H, and Wright, P. (2001), "Material Characterization of Fused Deposition Modeling (FDM) ABS by Designed Experiments," *Society of Manufacturing Engineers, Annual Conference*, pp. 1-21, Cincinnati, OH, April .

[4] Walish, J., Sutaria, M., Dougherty, M., Vaidyanathan, R., Kasichainula, S., and Calvert, P. (1999), "Application of Design of Experiments to Extrusion Freeform Fabrication (EFF) of Functional Ceramic Prototypes," *Solid Freeform Fabrication Conference*, Proceedings, pp. 103-110, Univ. of Texas, Austin, August.

[5] Ross, P.J. (1996), *Taguchi Techniques for Quality Engineering*, $2^{nd}$ Edition, McGraw-Hill.

[6] Summers, D.C. (1997), *Quality*, Prentice-Hall, Upper Saddle River, NJ.

[7] Gibson, R.F. (1994), *Principles of Composite Material Mechanics*, McGraw-Hill, Inc., New York.

[8] Montgomery,D.C., Runger, G.C., Hubele, N.F. (2000), *Engineering Statistics*, $2^{nd}$ Ed., J. Wiley & Sons, NY.

[9] Montgomery, D.C. (2001), *Design and Analysis of Experiments*, $5^{th}$ edition, John Wiley & Sons, Inc, New York.